

Feedforward and output feedback control of a highly oscillating and nonlinear 2-DOF piezoelectric actuator by using input shaping compensator and a linear quadratic regulator

Yasser AL HAMIDI^{1,2,*} and Micky RAKOTONDRABE¹

¹: Automatic Control and MicroMechatronic Systems (AS2M) dept of FEMTO-ST Institute UBFC, Université de Franche-Comté, ENSMM, CNRS, UTBM, 24, rue Alain Savary Besançon, France;

²: Texas AM University at Qatar, Doha, PO.Box 23874, Qatar

*: corresponding author: yasser.al-hamidi@qatar.tamu.edu

ABSTRACT

This paper deals with the control of a two degrees of freedom (2-DOF) piezoelectric cantilever actuator which is characterized by badly damped oscillations, hysteresis nonlinearity and cross-couplings. First, a feedforward control scheme based on the zero placement technique is introduced to annihilate the oscillations. Then a disturbance observer and a disturbance compensator are introduced to reduce the effects of low frequencies phenomena (hysteresis and creep) which were approximated by a fictive disturbance. Finally an output feedback scheme based on the linear quadratic regulator is added in order to reduce the cross-couplings effects to improve the tracking performances, and eventually to add robustness. Experiments were carried out and confirm the predicted performances.

Keywords: 2-DOF piezoactuator, cross-couplings, vibrations, badly damped oscillations, feedforward control, input shaping, disturbance observer, output-feedback control, LQR.

1. INTRODUCTION

Piezoelectric actuators (piezoactuators) are one of the most, if not the first, used actuators in micro and nanomanipulation, i.e. precise positioning ¹⁻⁴. The main reason is that they can offer a very high positioning resolution (down to nanometers) and a high bandwidth (in excess of the kHz). Additionally to that, piezoactuators are powered by electrical energy making their integration and use easier than purely thermal or other kinds of actuators. A classical type of piezoactuators used in micromanipulation and microassembly tasks is the piezoactuator with cantilever structure. Under a voltage excitation, it bends. This bending is afterwards exploited to push small objects. Furthermore, two piezoactuators with cantilever structure form a microgripper which can pick, transport and place the objects ^{5,6}. One of the principal advantages of piezoelectric microgripper is the possibility to control the manipulation force with one cantilever and the position with the other cantilever ⁷⁻⁹. Such active force and position control permits better performances and much more tasks possibility, contrary to position only or force only controlled microgrippers.

Cantilevered piezoactuators and piezoactuators in general are however typified by hysteresis and creep nonlinearities. These phenomena introduce loss of precision, though the high resolution. Furthermore, these nonlinearities may compromise stability of a closed-loop if they are not well accounted for during the controller design ⁵. In addition to hysteresis and creep nonlinearities, cantilever piezoactuators also exhibit badly damped oscillations due to the high Q-factor of the piezoelectric material and due to the cantilever structure itself. Vibrations induced during brusque input voltages are definitely unwanted in applications such as micromanipulation and microassembly because of the force overshoot that may destroy the objects and because of the risk of tasks instability. Also, badly damped oscillations lengthen the settling time of the actuator, even if it has a very short rise time, i.e. even if it has a large bandwidth. A major challenge in controlling badly damped system is the difficulty to design a feedback controller that can attenuate or even suppress the oscillations without increasing

the rise time, i.e. without degrading the bandwidth. Hence, instead of directly synthesizing a feedback controller, an efficient architecture consists in damping the vibrations with a feedforward controller first, and then adding a feedback to enhance the precision and the robustness. Different feedforward controllers techniques have been used to damp the vibrations in piezoactuators: linear time invariant model (LTI) direct inversion ¹⁰, input-shaping techniques ^{11,12}, H_∞ technique ^{13,14}, the zero error phase tracking control technique (ZEPTC) and the zero error magnitude tracking control technique (ZEMTC) ¹⁵, and nonlinear dynamics (hysteresis and dynamics) inversion techniques ¹⁶⁻¹⁸. These vibrations feedforward control could afterwards be augmented by a feedback scheme to improve the precision of the actuator or to add robustness against models uncertainties and disturbances ^{4,19-22}.

In recent years, a type of 2-DOF cantilevered piezoactuator has been designed and integrated in a 4-DOF gripper to perform dexterous tasks ²³. The 2-DOF actuator is characterized by strong vibrations, hysteresis and creep nonlinearities and cross-couplings between the axes. Different control scheme have been studied to improve the dynamic and static performances of such 2-DOF actuator, including feedforward only ^{13,24-26}, feedback only ^{27,28}, and feedforward-feedback combined ^{19,29}. In them, the feedback controllers are calculated such that the cross-couplings are considered as fictive disturbances and consequently the design problem comes back to a multiple SISO (single input single output) control problem. In this paper, we use MIMO (multiple input multiple output) model and controller synthesis. First in order to ease the feedback controller synthesis, we apply a MIMO vibrations feedforward control. Based on a MIMO input shaping technique developed in previous work, this permits to damp the first resonant frequency. Then we add a disturbance observer and a disturbance compensator to reduce the effects of a fictive disturbance which modeled the nonlinearities phenomena found at low frequency (hysteresis and creep). Finally, we suggest to augment the feedforward architecture by an output feedback synthesis in order to remove the cross-couplings effects and to enhance the tracking performances. This also permits to introduce robustness to the control systems. The output feedback is based on the linear quadratic regulator method and on a prefilter. Experimental tests demonstrate attaining the expected performances and the significance of the feedforward and output feedback combined control.

2. PRESENTATION AND CHARACTERIZATION OF THE 2-DOF PIEZOACTUATOR

2.1 The experimental setup

The 2-DOF piezoactuator is pictured in Fig. 1. When a voltage u_1 (resp. u_2) is applied for the actuator y_1 -axis (resp. y_2 -axis), a bending y_1 (resp. y_2) is obtained. These bendings can be exploited to perform small objects pushing. Furthermore, if two of the piezoactuator are used, a gripper capable of picking, transporting and releasing objects is obtained. The piezoactuator has 25mm of active length, 1mm of width and 1mm of thickness. To measure the bendings (displacements), two inductive sensors (ECL202 from IBS) are used. The sensors are tuned to have measurement resolution of tens of nanometers and a bandwidth in excess of 2kHz. The voltages and the measurement signals are generated and acquired by a computer with a dSPACE board embedding an ADC and DAC converters. The sampling time of the whole acquisition system is set to 50μs which is sufficient to consider all dynamics of the actuators and of the sensors.

2.2 Characterization

The static characteristics of the actuator were first studied. This is obtained by applying a sine input voltage u_1 (resp. u_2) to the piezoactuator with u_2 (resp. u_1) left equal to zero and by reporting the output displacements y_1 and y_2 . The amplitude is taken to be the maximal range of use (10V in this case) and the frequency is taken to be sufficiently low in order to avoid the phase-lag due to high dynamics, but not too low in order to avoid the creep effect ¹¹. Different experiments shown that a frequency of 0.1Hz is convenient for this actuator. Fig. 2-a depicts the output y_1 versus the input u_1 , i.e the (u_1, y_1) -plane, and Fig. 2-d depicts the (u_2, y_2) -plane. These two planes give the direct transfers of the 2-DOF piezoactuator which are clearly hysteretic. On the other hand, Fig. 2-b and Fig. 2-c depicts (u_2, y_1) -plane and the (u_1, y_2) -plane respectively and which are the cross-couplings

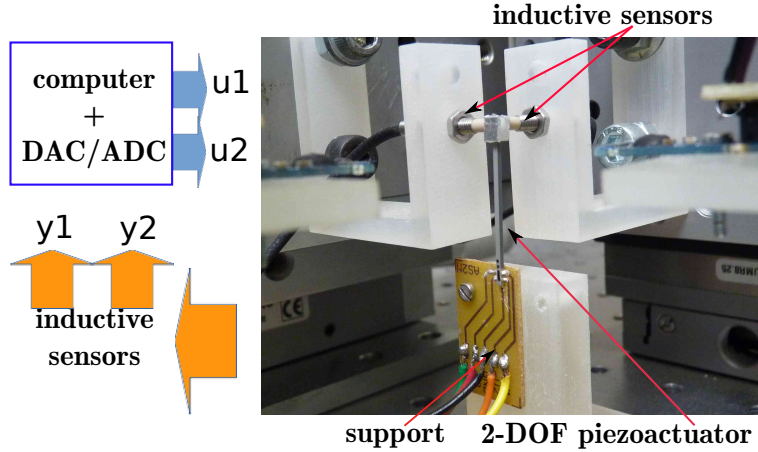


Figure 1: The 2-DOF piezoactuator and the experimental setup diagram.

of the actuator. The creep nonlinearity of the piezoactuator is evidenced when a step voltage is applied and the output y_1 or y_2 is observed during a long duration time. In this actuator, the creep is still evolving even several minutes after the step was applied. Fig. 2-e and h depict the direct creep characteristics of the actuator observed during 5min and Fig. 2-f and g depict the cross-couplings creep.

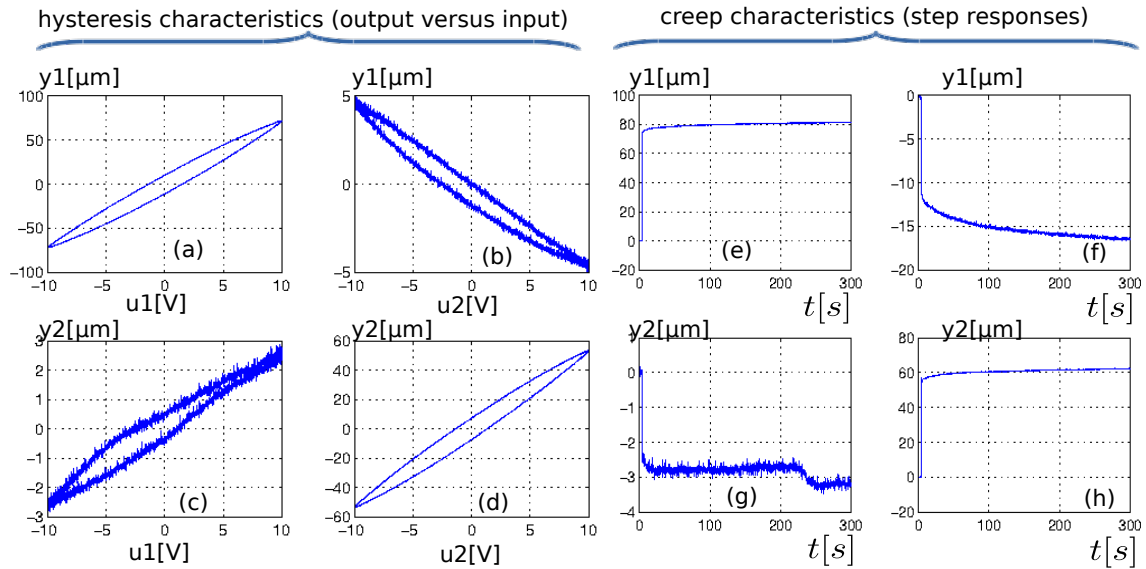


Figure 2: Low frequency and low-rate characteristics of the 2-DOF piezoactuator.

Finally, to characterize the dynamics, a step input voltage is applied. Then, the part of the step response before the creep starts is observed and can be used to identify this dynamics. Notice that both the creep and the transient part for the dynamics are observed from a step response. However, the creep is very low rate phenomena and thus observed during a long time duration whilst the dynamics is a very quick phenomena observed during tens or a hundred of millisecond. Fig. 3-a and d depict the transient parts (direct transfers) of the step responses of the actuator and Fig. 3-b and c correspond to the cross-couplings transient parts. As we can see, the actuators exhibit badly damped oscillations. As a consequence, the actuator possesses a very quick rise-time, however the settling time is very long relative to this.

2.3 Modeling and identification

In order to further synthesis a controller (feedforward and/or feedback), a model of the piezoactuator is essential. It was shown that a 1-DOF piezoactuator can be modelled by an uncertain linear model with fictive disturbance where the hysteresis and the creep are included in the uncertainties and in the disturbance ^{2, 27, 30, 31}. That is:

$$y(s) = G(s)u(s) + d(s) \quad (1)$$

where $G(s)$ is an uncertain linear transfer function, $d(s)$ is the disturbance and s is the Laplace variable.

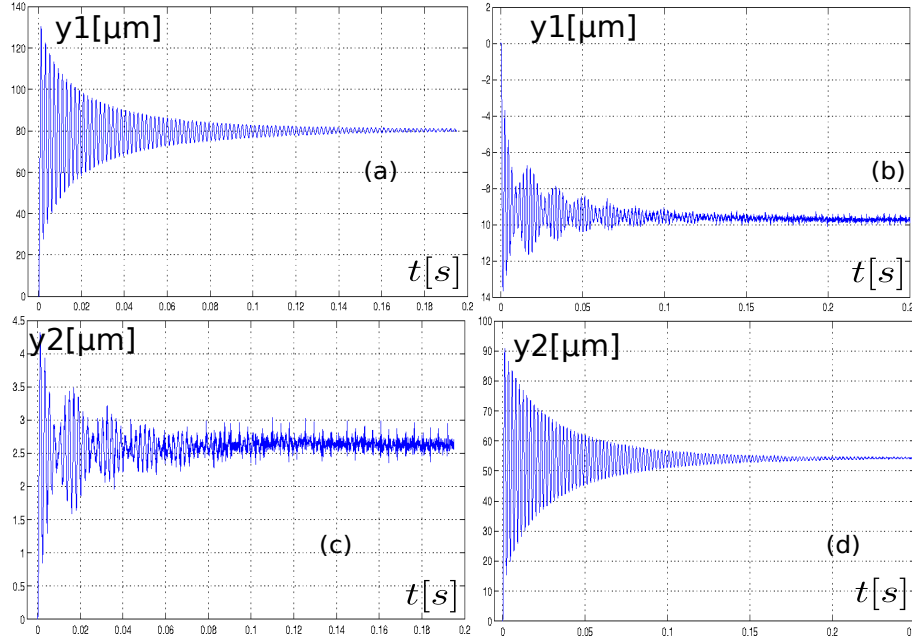


Figure 3: Step responses observed during a very short duration time.

By extending the 1-DOF model in (Eq 1) into 2-DOF, we have:

$$y(s) = \begin{pmatrix} y_1(s) \\ y_2(s) \end{pmatrix} = \begin{cases} G_1(s)u_1(s) + G_{12}(s)u_2(s) + d_1(s) \\ G_2(s)u_2(s) + G_{21}(s)u_1(s) + d_2(s) \end{cases} = G(s) \begin{pmatrix} u_1(s) \\ u_2(s) \end{pmatrix} + \begin{pmatrix} d_1(s) \\ d_2(s) \end{pmatrix} = G(s)u(s) + d(s) \quad (2)$$

where $G(s) = \begin{pmatrix} G_1(s) & G_{12}(s) \\ G_{21}(s) & G_2(s) \end{pmatrix}$. In our case, we will not consider the uncertainties in the model since a closed-loop controller will be introduced later. By applying a Box-Jenkins parametric identification technique to the experimental datas in Fig. 3 and by limiting the order of each transfer by four, we have:

$$\begin{cases} G_1(s) = \frac{-7881(s-9808)(s^2+309s+1.2 \times 10^7)}{(s^2+67s+1 \times 10^7)(s^2+933s+1.1 \times 10^7)} \\ G_{12}(s) = \frac{-777(s+21)(s^2+2319s+2 \times 10^7)}{(s+2181)(s+20)(s^2+84s+8 \times 10^6)} \\ G_{21}(s) = \frac{-88(s-3 \times 10^5)(s^2+7739s+3 \times 10^8)}{(s^2+349s+7 \times 10^6)(s^2+154s+4 \times 10^9)} \\ G_2(s) = \frac{-3140(s-1.3 \times 10^4)(s^2+680s+1 \times 10^7)}{(s^2+59s+8 \times 10^6)(s^2+1654s+1 \times 10^7)} \end{cases} \quad (3)$$

Transforming the 2-DOF model in (Eq 2) into a state-space model, we obtain:

$$\begin{cases} \frac{dx(t)}{dt} = Ax(t) + Bu(t) \\ y(t) = Cx(t) + d(t) \end{cases} \quad (4)$$

where the state matrix A , the input matrix B and the output matrix C , with appropriate dimensions, could be uncertain due to hysteresis and creep as mentioned above. The size of the state vector $x(t)$ is defined by the size of the matrix $G(s)$ which is itself defined during the identification procedure above. Fig. 4 presents the system.

In the next sections, we will first damp the vibrations (badly damped oscillations) *via* a feedforward control technique which will permit afterwards to ease the synthesis of a feedback controller.

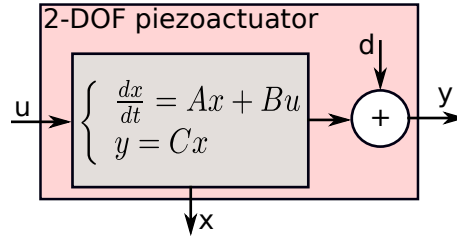


Figure 4: The system.

3. FEEDFORWARD CONTROL OF THE VIBRATIONS

The aim of this section is to damp the badly damped oscillations of the 2-DOF piezoactuator. A feedforward controller (also called compensator) based on the input shaping technique is proposed for that. In input shaping techniques, the compensator is particularly called shaper. Fig. 5-a depicts the block diagram of the system with the shaper. The next subsection will brief the method to synthesis this shaper. More details and an illustrative example are given in ²⁴.

3.1 Principle of the input shaping technique

Input shaping is a well-known feedforward technique to reduce vibrations in flexible structures. Input shapers typically alter the original input command by a longer shaped command that is convolved with a set of impulses. Input shaping has been given a great deal of attention for single input systems with a multiple modes of vibrations in time and frequency domains ³². For systems with multiple modes, shaped commands are typically constructed by cascading single-mode impulse sequences, hence a system with N modes of vibrations would need 3^N impulses shaper if individual shapers were 3-impulses ones. Although this approach is effective, shorter-length sequences would typically minimize distortion in the original command while eliminating all unwanted vibrations. As an alternate approach, reducing vibrations of multiple-mode systems can be done by placing zeros over all unwanted system poles in the z -plane. This technique allows shaper performance to be better tailored to specific system requirements and provides a conceptually simple and highly effective strategy for suppressing vibrations in flexible mechanical systems.

Similarly, input shapers for multi-input systems with multi-modes of vibrations can be designed using different methods. One method is to design all input shapers to be identical to each other and to be able to cancel out any mode of vibrations caused by the end of its input command ²⁴. This can be carried out by solving shaper constraint equations for only one sequence of impulses and apply it to all inputs. This method usually leads to relatively long time lags in the shaping sequence applied to all inputs, especially for large complex flexible structures with many flexible modes. Another method which generally leads to a shorter sequences, is to include more information about the flexible system model into the problem formulation and solving for the impulse sequences simultaneously. In this case, the problem of coupling among inputs is addressed by including information from the input matrix B of the system model into the derivation of the designed shapers.

For a system with $m + 1$ input, single output, and n structural frequencies w_1, \dots, w_n , the transfer matrix from the unshaped inputs to the system states, including the shaper, is $(sI - A)^{-1} BQ(s)$ where the multiple input shaper transfer functions are $Q_r(s)$, $r = 0, 1, 2, \dots, m$ and $Q(s)$ is a vector containing them. To filter out any vibrations due to the flexible mode, we choose $Q_r(s)$ such that:

$$b_0^i Q_0(s) + b_1^i Q_1(s) + \dots + b_m^i Q_m(s) \Big|_{s=-i w_i \pm j w_{i,d}} = 0 \quad (5)$$

where $A = \text{blockdiag} \begin{bmatrix} 0 & 1 \\ -w_i^2 & -2\xi w_i \end{bmatrix}$, $B = \text{blockcol} \begin{bmatrix} 0 & 0 & \dots & 0 \\ b_0^i & b_1^i & \dots & b_m^i \end{bmatrix}$, $i = 0, 1, 2, \dots, n$ and $Q_r(s) = a_{0r} + a_{1r}e^{-sT} + \dots + a_{lr}e^{-s l T}$.

This same approach can be applied and extended to multiple output systems if we separated the multi-input multi-output system (MIMO) into different number of systems equal to the number of outputs. Each of the resulting systems has the same number of inputs as the original system and only one output. However to be able to have one solution of all input shapers for all outputs, we have to include B_j information for all outputs in the shaper design process. That is, the designed shapers should be able to cancel all modes of vibrations for all outputs. The new input matrix $B = \text{Blockcol} [B_j] = \text{Blockcol} \left[B = \text{blockcol} \begin{bmatrix} 0 & 0 & \dots & 0 \\ b_{j0}^i & b_{j1}^i & \dots & b_{jm}^i \end{bmatrix} \right]$ where $i = 0, 1, 2, \dots, n$ is the number of structural frequencies in each direction and $j = 1, 2, \dots, k$ is the number of outputs.

3.2 Compensation results

The shaper briefly presented in the previous subsection has been calculated with the identified parameters of the model in (Eq 4), and then implemented. Only the first resonance has been studied, identified and compensated for the two axes which is sufficient for the focused applications. Fig. 5-b shows the detailed scheme of the shaper which is composed of two "sub"-shapers for the two input voltages u_1 and u_2 . In the figure, u_{s1} and u_{s2} are the shaped input voltages. Fig. 5-c show the step responses simulation with and without the calculated compensator. They clearly show the substantial damping of the vibrations when the compensator is implemented.

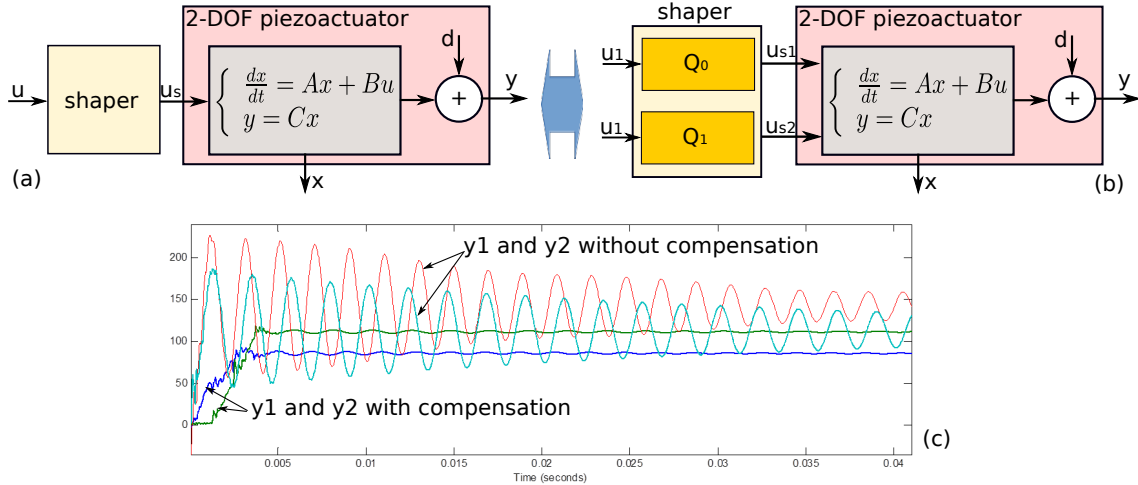


Figure 5: (a): the system with the vibrations compensator (shaper). (b): the detailed shaper. (c): simulation results.

4. LQR FEEDBACK CONTROL

The previous section dealt with the damping of the badly damped oscillations of the 2-DOF piezoactuator by using a feedforward controller based on a MIMO input shaping technique presented in ²⁴. In this section, we augment the previous scheme by a feedback controller in order to remove the cross-couplings effects and to introduce a good tracking performance. An interest of the feedback is also its robustness relative to feedforward.

4.1 The new system

The system to be controlled by the feedback scheme is the compensated system of input u and of output y as presented in Fig. 5. This system has a new dynamics as well as a new static parts relative to the initial model in (Eq 4). Since the output disturbance $d(s)$ which encloses the hysteresis and the creep nonlinearities is a low frequency signal, and since the piezoactuator dynamics has a high frequency characteristics, it is possible to move $d(s)$ at the input (input disturbance) where it is still dominant. In order to maintain the generalization, let us name this input disturbance $b(s)$, instead of $d(s)$. Therefore Fig. 6 depicts the equivalence of Fig. 5 when translating the output disturbance at the input. Also, the new model becomes:

$$\Sigma_{ff} : \begin{cases} \frac{dx(t)}{dt} = A_{ff}x(t) + B_{ff}u(t) + B_{ff}b(t) \\ y(t) = C_{ff}x(t) \end{cases} \quad (6)$$

where A_{ff} , B_{ff} and C_{ff} are the new state, input and output matrices respectively which are based on A , B and C and on the shaper.

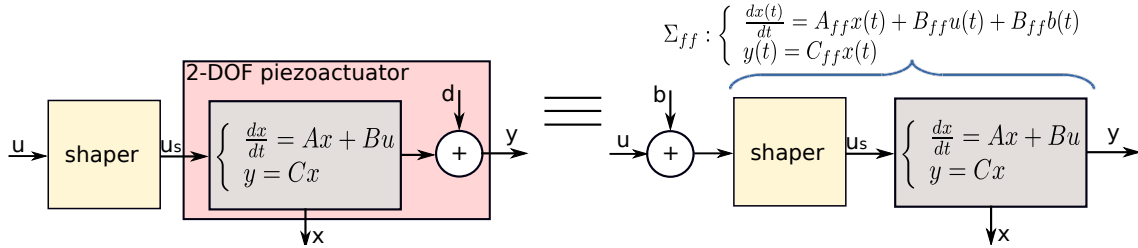


Figure 6: Translating the output disturbance d at the input.

4.2 DOB and disturbance rejection

In order to further study an output feedback controller, we propose first to remove the input disturbance b from the feedback. For that a disturbance observer (DOB) is first suggested. The estimate $\hat{b}(s)$ is afterwards used as a negative feedback such that we have $u + b - \hat{b} = u$ as input of the shaper, see Fig. 7-a. In this case, the system to be controlled by the output feedback controller is without the disturbance b . The DOB is based on the technique proposed in ³³ where $F(s)$ is a filter conveniently chosen for robustness and Σ_{ff} should be identified in a such a way it is minimum phase.

4.3 The LQR controller design

We now use the system with the shaper and with the DOB to construct and to synthesize the output feedback controller. The controller is composed of the output feedback gain K and the prefilter L , see Fig. 7-b. Remind that the reason why we removed the disturbance b thanks to the DOB is to automatically reject this disturbance in the closed-loop. In other word, to obtain $y = y_r$ in steady-state regime whatever b is, where y_r is the reference input. Without this DOB, and thus without removing $b(s)$, there would have been a statical error with this output feedback controller to be designed.

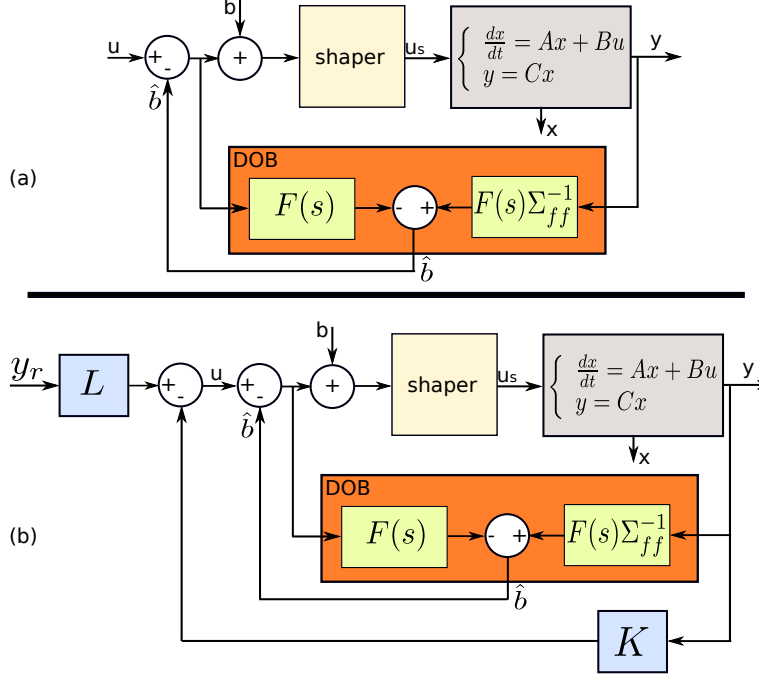


Figure 7: (a): introduction of a DOB to remove the input disturbance $b(s)$. (b): an output feedback control scheme.

From the model in (Eq 6) and the block-diagram in Fig. 7-b, with consideration of the DOB effect, we have the following governing equations:

$$\begin{cases} \frac{dx}{dt} = A_{ff}x + B_{ff}u \\ y = C_{ff}x \\ u = Ly_r - Ky \end{cases} \quad (7)$$

which, after rearrangement, implies the model of the closed-loop:

$$\begin{cases} \frac{dx}{dt} = (A_{ff} - B_{ff}KC_{ff})x + B_{ff}Ly_r \\ y = C_{ff}x \end{cases} \quad (8)$$

Thus, K can be designed to impose the dynamics of the closed-loop which is defined by the state matrix $(A_{ff} - B_{ff}KC_{ff})$. For that we use the linear quadratic regulator principle (LQR). Consider the following (quadratic) performance index:

$$J = \int_0^{\infty} (y^T Q_y y + u^T R u) dt \quad (9)$$

where Q_y and R are diagonal and positive semi-definite matrices that weight the elements of y and u respectively according to their importance in the control problem. The two matrices can also be used to weight in a global manner the input relative to the output or conversely. The objective is to find the feedback gain K such that the cost J is minimized, i.e. the output transient part energy and the input energy are minimized. Introducing $y^T = x^T C^T$ and $y = Cx$ in (Eq 9), the problem becomes in finding K such that the following J is minimized:

$$J = \int_0^{\infty} (x^T Q x + u^T R u) dt \quad (10)$$

where $Q = C^T Q_y C$ is diagonal and positive semi-definite.

Solving the LQR problem for output feedback architecture is not as direct as that of LQR problem in state-feedback architecture. The optimal gain design K is derived from the following equations ³⁴.

$$\begin{aligned} 0 &= A_{cl}^T P + P A_{cl} + C_{ff}^T K^T R K C_{ff} + Q \\ 0 &= A_{cl} S + S A_{cl}^T + X \\ K &= R^{-1} B_{ff}^T P S C_{ff}^T \left(C_{ff} S C_{ff}^T \right)^{-1} \end{aligned} \quad (11)$$

where $A_{cl} = A_{ff} - B_{ff} K C_{ff}$, $X = E\{x(0)x^T(0)\}$, P is the solution of the first equation in (Eq 11) and S is the solution of the second one. The initial autocorrelation of the state X is usually unknown because the initial state $x(0)$ is unknown. In this case, we take the maximal range of the state $x(t)$ when applying the maximal voltage step (10V) as initial values. They are taken from the simulation of the model Σ_{ff} . The resolution of the equations in the design problem in (Eq 11) is carried out with the numerical algorithm in ³⁴.

The previous calculation permitted to obtain the feedback gain K . To obtain the prefilter L , the steady-state regime is first calculated. For that, we let $\frac{dx(t)}{dt} = 0$ in (Eq 8). We have:

$$y = C_{ff} (B_{ff} K C_{ff} - A_{ff})^{-1} B_{ff} L y_r \quad (12)$$

To make $y = y_r$ at the steady-state regime, from (Eq 12), one should have:

$$C_{ff} (B_{ff} K C_{ff} - A_{ff})^{-1} B_{ff} L = I \Leftrightarrow L = \left(C_{ff} (B_{ff} K C_{ff} - A_{ff})^{-1} B_{ff} \right)^{-1} \quad (13)$$

4.4 Experimental results

The calculated controller has been implemented. First we apply a step reference input $y_{1r} = 60\mu s$ along y_1 axis. Then, later, we apply a step reference input $y_{2r} = 60\mu s$ along y_2 axis. Fig. 8-a depicts the response of y_1 relative to these step inputs while Fig. 8-b is the response of y_2 . As we can see, the output y_1 directly reaches the reference y_{1r} (at about 2.4s) and the static error is always maintained zero afterwards. The application of the reference y_{2r} at about 5.45s provokes a slight disturbance (cross-coupling) to y_1 but this is quickly rejected. The same performance is also found for y_2 : the disturbance (cross-coupling) due to the application of the step y_{1r} at about 2.4s is quickly rejected, and the output y_2 quickly reaches the reference y_{2r} at about 5.45s. These results also show that the static error is maintained negligible which show the efficiency of the DOB to remove low frequency (internal) disturbance effect. Without this DOB and disturbance rejection, the hysteresis and the creep would have affected the static error.

The previous results have been zoomed and are shown in Fig. 9. Fig. 9-a shows the step response of y_1 and Fig. 9-d shows the step response of y_2 . The settling time is less than 20ms for both. They also show the strongly damped oscillations relative to the responses of the initial system (see Fig. 3). This is thanks to the input shaping technique augmented by the feedback controller. Without the input shaping technique, it would have been difficult to find the feedback controller able to reduce the oscillations with simultaneously such settling time. Notice that the settling time of the initial system (see Fig. 3) was about 100ms. Finally Fig. 9-b and c shows the cross-couplings rejections which are very quick thanks to the feedback controller.

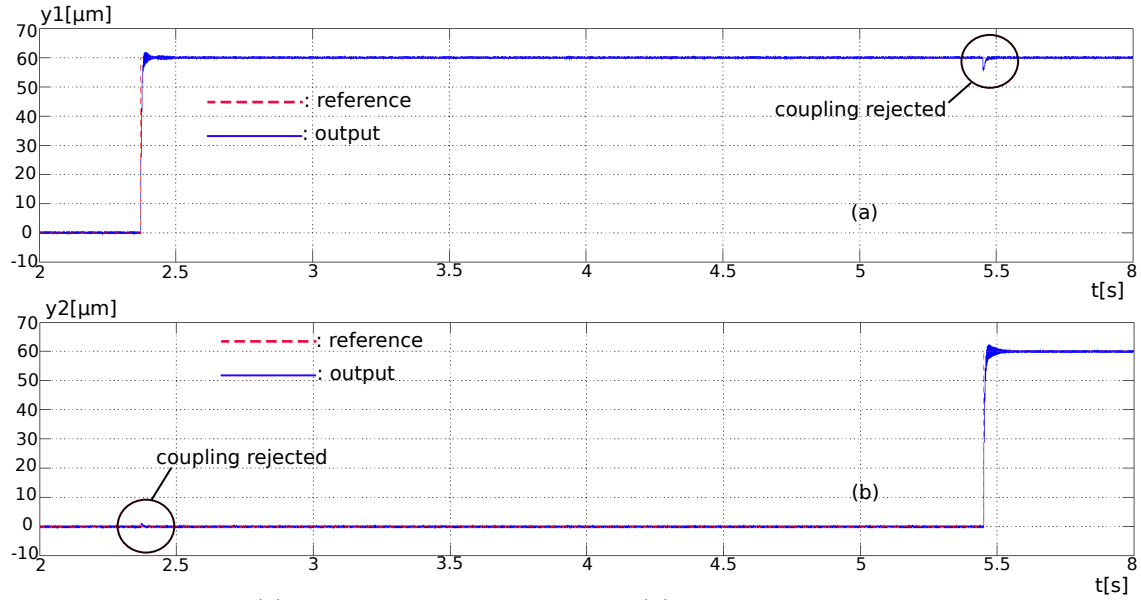


Figure 8: (a): step response along y_1 axis. (b): step response along y_2 axis.

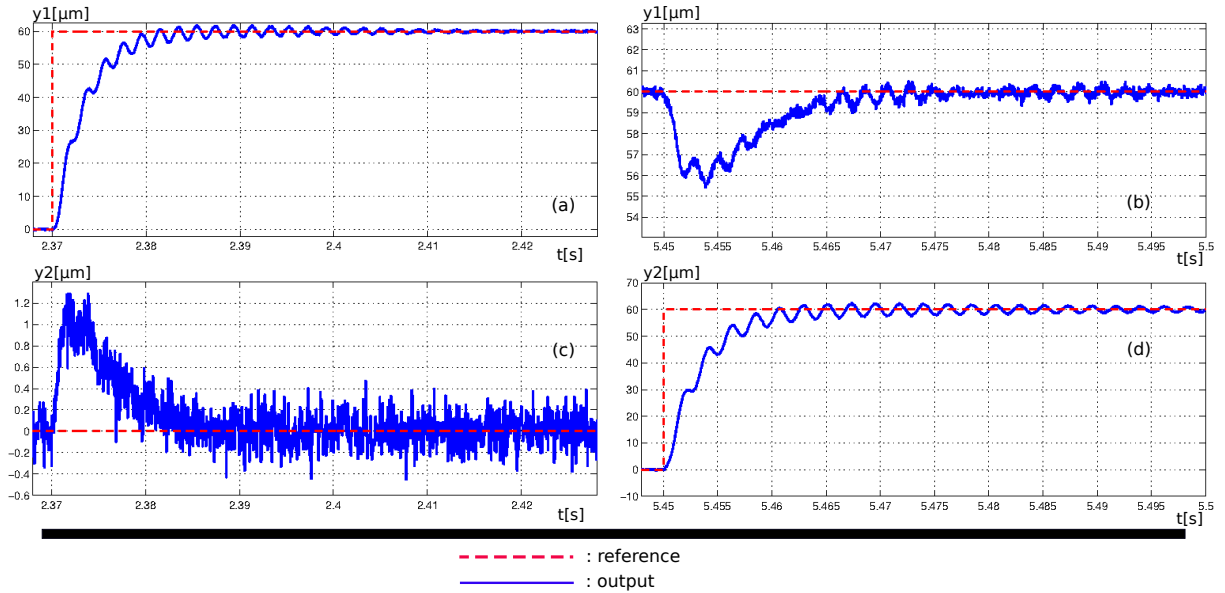


Figure 9: Zoom of the different step responses.

5. CONCLUSIONS

This paper dealt with the control of a 2-DOF oscillating and nonlinear piezoactuator. First the linear model with fictive disturbance that accounts for the nonlinearities and the cross-couplings is expressed. Then, a feedforward controller based on a MIMO input shaping technique is applied to the actuator in order to damp the vibrations. The calculation of the shaper (vibrations compensator) is based on the model expressed. In order to remove the fictive distortion, we afterwards implement a disturbance observer and an input disturbance compensation. Finally, an output feedback controller based on a feedback gain and a prefilter is calculated and implemented. The experiments show the efficiency of the whole architecture to damp the vibrations, to reject the effect of the nonlinearities in the precision of the actuator and to have a convenient tracking rapidity.

6. ACKNOWLEDGMENTS

This work was supported by the national ANR-JCJC C-MUMS-project (National young investigator project ANR-12-JS03007.01: Control of Multivariable Piezoelectric Microsystems with Minimization of Sensors). This work was also supported by the LABEX ACTION (ANR-11- LABX-0001-01)..

REFERENCES

- [1] J. Agnus, N. Chaillet, C. Clévy, S. Dembélé, M. Gauthier, Y. Haddab, G. Laurent, P. Lutz, N. Piat, K. Rabenorosoa, M. Rakotondrabe and B. Tamadazte, "Robotic microassembly and micromanipulation at FEMTO-ST," *Journal of Micro-Bio Robotics*, vol. 8, no. 2, pp. 91-106, 2013.
- [2] M. Rakotondrabe, *Smart materials-based actuators at the micro/nano-scale: characterization, control and applications*, Springer-Verlag, NewYork, 2013.
- [3] S. Devasia, E. E. Eleftheriou, R. Moheimani, "A survey of control issues in nanopositioning", *IEEE Transactions on Control Systems Technology*, Vol.15, N°5, pp.802-823, 2007.
- [4] M. Rakotondrabe, 'Piezoelectric systems for precise and high dynamic positioning: design, modeling, estimation and control', HDR halititation thesis, University of Franche-Comt / FEMTO-ST, November 10, 2014.
- [5] Y. Haddab, N. Chaillet, A. Bourjault, "A microgripper using smart piezoelectric actuators", *IEEE International Conference on Intelligent Robots and Systems*, 2000.
- [6] J. Agnus, P. Nectoux, N. Chaillet, "Overview of microgrippers and design of a micromanipulation station based on a MMOC microgripper", *IEEE International Symposium on Computational Intelligence in Robotics and Automation*, 2005.
- [7] M. Rakotondrabe and A. Ivan, 'Development and Force/Position Control of a New Hybrid Thermo-Piezoelectric microGripper dedicated to micromanipulation tasks', *IEEE Transactions on Automation Science and Engineering*, 8(4), pp.824-834, October 2011.
- [8] S. Khadraoui, M. Rakotondrabe and P. Lutz, 'Interval force/position modeling and control of a microgripper composed of two collaborative piezoelectric actuators and its automation', *International Journal of Control, Automation and Systems*, 12(2), Page 358-371, April 2014.
- [9] M. Rakotondrabe, C. Clévy and P. Lutz, 'Modelling and robust position/force control of a piezoelectric microgripper', *IEEE International Conference on Automation Science and Engineering*, Scottsdale AZ USA, 2007.
- [10] D. Croft, G. Shed and S. Devasia, "Creep, hysteresis and vibration compensation for piezoactuators: atomic force microscopy application", *ASME Journal of Dynamic Systems, Measurement and Control*, 2001.
- [11] M. Rakotondrabe, Cédric Clévy and P. Lutz, 'Complete open loop control of hysteretic, crepted and oscillating piezoelectric cantilever', *IEEE Transactions on Automation Science and Engineering*, Vol.7(3), pp:440-450, July 2010.
- [12] M. Rakotondrabe, Cédric Clévy and P. Lutz, 'Hysteresis and vibration compensation in a nonlinear unimorph piezocantilever', *IEEE International Conference on Intelligent Robots and Systems*, pp:558-563, Nice France, Sept 2008.
- [13] D. Habineza, M. Rakotondrabe and Y. Le Gorrec, ' Simultaneous Suppression of Badly-Damped Vibrations and Cross-couplings in a 2-DoF piezoelectric actuator, by using Feedforward Standard H-inf approach', *SPIE Sensing Technology+Applications; Sensors for Next Generation Robots conference* , 9494-29, Baltimore Maryland USA, April 2015.
- [14] G. Schitter, A. Stemmer, F. Allgower, "Robust 2 DOF-control of a piezoelectric tube scanner for high speed atomic force microscopy", *American Control Conference*, pp. 3720-3725, June 2003.
- [15] J.A. Butterworth, L.Y. Pao and D.Y. Abramovitch, "A Single-Parameter Combined Feedforward/Feedback Adaptive-Delay Algorithm with Applications to Piezo-Based Raster Tracking", *IEEE Transactions on Control Systems Technology*, 20(2), 2011.
- [16] M. Al Janaideh, M. Rakotondrabe and O. Al Janaideh, 'Further Results on Hysteresis Compensation of Smart Micro-Positioning Systems with the Inverse Prandtl-Ishlinskii Compensator', *IEEE Transactions on Control Systems Technology*, doi:10.1109/TCST.2015.2446959, 2016.

- [17] O. Aljanaideh, D. Habineza, M. Rakotondrabe and M. Al Janaideh, 'Experimental comparison of rate-dependent hysteresis models in characterizing and compensating hysteresis of piezoelectric tube actuators', Elsevier Physica B: Condensed Matter, doi:10.1016/j.physb.2015.10.021, oct 2015.
- [18] W. T. Ang, P. K. Kholsa and C. N. Riviere, Feedforward controller with inverse rate-dependent model for piezoelectric actuators in trajectory-tracking applications, IEEE/ASME Transactions on Mecha- tronics, Vol.12(2), pages 134-142, April 2007.
- [19] M. Rakotondrabe, K. Rabenoroso, J. Agnus and N. Chaillet, 'Robust feedforward-feedback control of a nonlinear and oscillating 2-dof piezocantilever', IEEE Transactions on Automation Science and Engineering, 8(3), pp.506-519, July 2011.
- [20] K. K. Leang and S. Devasia, "Feedback-linearized inverse feedforward for creep, hysteresis, and vibration compensation in AFM piezoactuators", IEEE Trans. Control Syst. Technol., vol. 15, no. 5, pp. 927935, Sep. 2007.
- [21] J. A. Butterworth, L. Y. Pao, and D. Y. Abramovitch, "Architectures for tracking control in atomic force microscopes", in Proc. IFAC World Congr., 2008, pp. 82368250.
- [22] Po-Jen Koa, Yen-Po Wang, Szu-Chi Tien, "Inverse-feedforward and robust-feedback control for high-speed operation on piezo-stages", International Journal of Control, Vol.86(2), 2013.
- [23] P. de Lit, J. Agnus, C. Clévy and N. Chaillet, A four-degree-of-freedom microprehensile microrobot on chip, International Journal of Assembly Technology and Management (Assembly Automation), 2004.
- [24] Y. Al Hamidi and M. Rakotondrabe, 'Multi-Mode Vibration Suppression in 2-DOF Piezoelectric Systems Using Zero Placement Input Shaping Technique', SPIE Sensing Technology+Applications; Sensors for Next Generation Robots conference , 9494-27, Baltimore Maryland USA, April 2015.
- [25] D. Habineza, M. Rakotondrabe and Y. Le Gorrec, 'Bouc-Wen Modeling and Feedforward Control of multi-variable Hysteresis in Piezoelectric Systems: Application to a 3-DoF Piezotube scanner', IEEE Transactions on Control Systems Technology, Vol 23, Issue 5, Page 1797-1806, Sept 2015.
- [26] M. Rakotondrabe, 'Modeling and Compensation of Multivariable Creep in multi-DOF Piezoelectric Actua- tors', IEEE International Conference on Robotics and Automation, pp.4577-4581, St Paul Minnesota USA, May 2012.
- [27] D. Habineza, M. Rakotondrabe and Y. Le Gorrec, 'Characterization, Modeling and H-inf Control of n- DOF Piezoelectric Actuators: Application to a 3-DOF Precise Positioner', Asian Journal of Control, DOI=10.1002/asjc.1224, Vol. 18, No. 5, pp. 1-20, September 2016.
- [28] J.A. Escareno, M. Rakotondrabe and D. Habineza, 'Backstepping-based robust-adaptive control of a non- linear 2-DOF piezoactuator', IFAC - Control Engineering Practice (CEP), Vol.41, Pages 57-71, August 2015.
- [29] M. Rakotondrabe, J. Agnus and P. Lutz, 'Feedforward and IMC-feedback control of a nonlinear 2-DOF piezoactuator dedicated to automated micropositioning tasks', IEEE International Conference on Automa- tion Science and Engineering, pp.393-398, Trieste Italy, August 2011.
- [30] M. Rakotondrabe, Y. Haddab and P. Lutz, 'Plurilinear modeling and discrete -synthesis control of a hysteretic and creeped unimorph piezoelectric cantilever', IEEE International Conference on Automation, Robotics, Control and Vision, pp:57-64, Grand Hyatt Singapour, December 2006.
- [31] M. Rakotondrabe, Y. Haddab and P. Lutz, 'Quadrilateral modelling and robust control of a nonlinear piezoelectric cantilever', IEEE Transactions on Control Systems Technology, 17(3), pp:528-539, May 2009.
- [32] L.Y. Pao, "Multiple Input-Shaping Design for Vibration Reduction", Automatica, 35, pp. 8 1-89, January 1999.
- [33] A.E. El-Shaer, M. Al Janaideh, P. Krejci and M. Tomizuka, "Robust Performance Enhancement Using Disturbance Observers for Hysteresis Compensation Based on Generalized PrandtlIshlinskii Model", ASME Journal of Dynamic Systems, Measurement, and Control, 135, 2013.
- [34] F.L. Lewis, D. Vrabie, V.L. Syrmos, "Optimal control", Wiley, ISBN: 978-0-470-63349-6, 2012.